Articles

Folded State of the Integral Membrane Colicin E1 Immunity Protein in Solvents of Mixed Polarity[†]

Ross M. Taylor,[§,‡,⊥] Stanislav D. Zakharov,[§,‡,||] J. Bernard Heymann,[‡,#] Mark E. Girvin,[¶] and William A. Cramer*[,‡]

Department of Biological Sciences, Purdue University, West Lafayette, Indiana 47907, Institute of Basic Research, Russian Academy of Sciences, Pushchino, Russia, Department of Biochemistry, Albert Einstein College of Medicine, Bronx, New York 10461

ABSTRACT: The colicin E1 immunity protein (ImmE1), a 13.2-kDa hydrophobic integral membrane protein localized in the *Escherichia coli* cytoplasmic membrane, protects the cell from the lethal, channel-forming activity of the bacteriocin, colicin E1. Utilizing its solubility in organic solvents, ImmE1 was purified by 1-butanol extraction of isolated membranes, followed by gel filtration and ion-exchange chromatography in a chloroform/methanol/H_2O (4:4:1) solvent system. Circular dichroism analysis indicated that the α-helical content of ImmE1 is approximately 80% in 1-butanol or 2,2,2-trifluoroethanol, consistent with a previous membrane-folding model with three extended hydrophobic transmembrane helical domains, H1−H3. Each of these extended hydrophobic domains contains a centrally located single Cys residue that could be used as a probe of protein structure. The presence of tertiary structure of purified ImmE1 in a solvent of mixed polarity, chloroform/methanol/H_2O (4:4:1) was demonstrated by (i) the constraints on Tyr residues shown by the amplitude of near-UV circular dichroism spectra in the wavelength interval, 270−285 nm; (ii) the correlation between the near-UV Tyr CD spectrum of single and double Cys-to-X mutants of the Imm protein and their in vivo activity; (iii) the upfield shift of methyl groups in a 1D NMR spectrum, a 2D- HSQC NMR spectrum of ImmE1 in the mixed polarity solvent mixture, and a broadening and disappearance of the indole ^{1}H proton resonance from Trp94 in H3 by a spin label attached to Cys16 in the H2 hydrophobic domain; (iv) near-UV circular dichroism spectra with a prominent ellipticity band centered at 290 nm from a single Trp inserted into the extended hydrophobic domains. It was concluded that the colicin E1 immunity protein adopts a folded conformation in chloroform/methanol/ H_2O (4:4:1) that is stabilized by helix−helix interactions. Analysis of the probable membrane folding topology indicated that several Tyr residues in the bilayer region of the three transmembrane helices could contribute to the near-UV CD spectrum through helix−helix interactions.

Colicin E1 is a plasmid-encoded toxin, produced by and active against *Escherichia coli* cells, which exerts its cytotoxicity by forming a highly conductive ion channel in the cytoplasmic membrane of susceptible strains (*1*). The efficiency of the colicin is rivaled by that of its immunity protein (ImmE1),[1] which is encoded on the same plasmid and protects colicin-producing strains against concentrations of the toxin 10^4-10^7 times higher than that required to kill nonimmune cells (*2*). The immunity gene is present for self-preservation in plasmids coding bacteriocins that are cytotoxic toward sister cells (*3*). No protein analogous to Imm is present in bacteria producing toxins that act on foreign eukaryotic cells. Inhibition of productive channel formation by colicin E1 has been proposed to occur through specific and direct interaction between the helices of the colicin channel-forming domain and ImmE1 within the membrane bilayer (*4*), but it has not yet been possible to test the existence, nor to understand the structural basis, of such interactions. For this purpose, it is necessary to overexpress, purify, and ultimately gain high-resolution structure informa-

* To whom correspondence should be addressed. Telephone: 765-494-4956; fax: 765-496-1189; e-mail: wac@bilbo.bio.purdue.edu.
[§] Senior authors.
[‡] Purdue University.
[||] Russian Academy of Sciences.
[¶] Albert Einstein College of Medicine.
[⊥] Present address: Department of Microbiology, Montana State University, Bozeman, MT 59717.
[#] Present address: LSBR, NIAMS, Bldg 6, 6 Center Drive, MSC 2717, National Institutes of Health, Bethesda, MD 20892-2717.

[1] Abbreviations: BR, bacteriorhodopsin; CD, circular dichroism; DAGK, diacylglycerol kinase; DMG, dimethyglutaric acid; DTT, dithiothreitol; Emr, *E. coli* multidrug resistance transport protein; HSQC: heternuclear single quantum correlation; H1, H2, H3, extended hydrophobic domains, trans-membrane helices, 1, 2, 3; ImmE1, colicin E1 immunity protein; NMR, nuclear magnetic resonance; PCR, polymerase chain reaction; PMSF, phenylmethanesulfonylfluoride; SDS, sodium dodecyl sulfate; TFE, 2,2,2-trifluoroethanol.

tion for the integral membrane immunity protein in a membrane-mimetic environment.

The isolation and high-resolution structure determination of integral membrane proteins provides challenges, due to the requirements of finding suitable detergent conditions for solubilization and purification and in generating high-resolution three-dimensional crystals from detergent-solubilized membrane proteins (5, 6). For a limited number of hydrophobic integral membrane proteins, efficient purification (7−11) and structure determination by NMR spectroscopy with varying degrees of success (12−15) have exploited the unique solubility of certain small membrane proteins in organic solvents.

The potential utility of such solvent systems for structural analysis has been demonstrated in studies on the integral membrane proteins DAGK (14), EmrE (16), and a bacteriorhodopsin fragment (17). Highly helical secondary structures observed in organic solvents proved consistent with predictions based on primary sequence (16, 18, 19) and spectroscopic analysis following reconstitution into artificial membranes (16, 20, 21). Unfortunately, little or no evidence for tertiary folding was found in these cases.

For subunit c of F_1F_o ATP synthase, a small bitopic integral membrane protein, tertiary structure, native folding, and functionally relevant conformational changes were observed in chloroform/methanol/water mixtures. Tertiary folding was demonstrated by long-range, interhelix interactions between spin labels introduced in one helix on the relaxation properties of residues in the neighboring helix (22, 23). The complete three-dimensional structure was subsequently determined by NMR at low pH where the proton-transferring Asp61 side chain is protonated (12). This structure was consistent with both the long-range interactions within monomers predicted from mutagenesis experiments and patterns of contacts between monomers identified by disulfide cross-linking experiments (24). Furthermore, the structure of the Asp61-deprotonated form of the protein was subsequently solved (25). This second conformation was consistent with cross-linking data between subunit c and subunit a of the F_o complex (26). The observed conformational changes have provided a basis for the mechanism of coupling of proton transfer through subunit c to γ subunit rotation and rotational coupling of ATP synthesis within the ATP synthase (25). Thus, for subunit c of the integral membrane protein F_o complex of the ATP synthase, a chloroform/methanol/water solvent system appears to be membrane-mimetic. The special properties of this solvent mix may be a consequence of the demonstrated preferential solvation by methanol and chloroform of the hydrophilic and hydrophobic parts of amphiphilic solutes (27). Relevant properties of the proteins that have been analyzed structurally to at least some extent in this solvent system are summarized (Table 1).

In contrast to the situation with the proteolipid subunit c, it has not been possible to show that the other small hydrophobic proteins or peptides summarized in Table 1 can assume a native conformation in organic solvents. Thus, the general utility of organic solvents for structure determination of integral membrane proteins by NMR spectroscopy has not been demonstrated. The ability of organic solvents to mimic the natural environment of a biological membrane is not known. Further examples of integral membrane proteins

Table 1: Physical Properties of Integral Membrane Proteins Purified and Characterized in Organic Solvents

protein	MW (kDa)	pI[a]	charged res (%)	net charge	hydrophob index[b]
ImmE1	13.2	9.36	15.0	+7	0.63
EmrE	12.0	7.72	6.3	+1	1.05
diacyglycerol kinase	13.2	6.05	17.0	−1	0.88
subunit c of ATP-synthase	8.3	4.44	10.1	−2	1.3
1−71 fragment of BR[c]	7.7	8.80	11.2	+2	0.75
phospholamban	6.1	9.15	13.4	+3	0.84
P190[d]	23.0	8.92	25.2	+4	−0.1

[a] Isoelectric point. [b] Calculations based on a hydrophobicity scale with values ranging from −4.5 for least hydrophobic to 4.5 for most hydrophobic (33). [c] N-terminal 71-residue fragment of bacteriorhopsin (15). [d] The colicin E1 channel domain, a soluble protein, which is insoluble in both 1-butanol and chloroform/methanol/H_2O solvent systems, listed for the purpose of comparison.

that retain solubility in a variety of membrane-mimetic environments are required to determine whether there is a group of proteins that reliably folds into native structures in organic solvents or, alternatively, resembles the "alcohol-denatured" state of soluble proteins, characterized by the presence of secondary structure elements in the absence of specific tertiary contacts (28−32).

The ImmE1 immunity protein for colicin E1 was purified by a rapid and efficient isolation procedure based on its unique solubility in organic solvents. Using CD and NMR spectroscopies, it was found that ImmE1 in solvents of mixed polarity assumes a folded conformation with significant tertiary structure.

EXPERIMENTAL PROCEDURES

Reagents. 1-Butanol, chloroform, and methanol (analytical grade) were obtained from Mallinckrodt. Sephadex LH-20-100, CM-cellulose, and SDS were from Sigma, 3-maleimido-PROXYL from Aldrich, low molecular weight protein standards from BioRad, and $^{15}NH_4Cl$ was from Cambridge Isotope Laboratory.

Construction and Mutation of pT7Imm. The immunity protein gene, *imm,* was cloned behind the T7 promoter to facilitate overexpression. The *Eco*RI/*Bam*HI fragment of pColE1 coding for the immunity protein was cloned into M13mkp18. The *Nde*I restriction site was inserted before the start codon of *imm* gene, and the 0.4 kb *Nde*I/*Eco*RI fragment was cloned into pT7-7 to produce pT7Imm. The wild-type ImmE1 was expressed from pT7Imm in the *E. coli* strains BL21(DE3).

A modified PCR-based protocol (34) was used to generate mutations in pT7Imm. Two mutagenic oligonucleotide primers, complementary to opposite strands of the vector, were extended during PCR using *Pfu* DNA polymerase (Stratagene). The reaction mixture after PCR was treated with *Dpn*I to digest the parental DNA template resulted in selection for synthesized strand with the mutation. Epicurian XL1-Blue *E. coli* cells (Stratagene) were transformed with *Dpn*I-treated PCR mixture. Mutagenized pT7Imm was isolated from the cells propagated from ampicillin-resistant colonies and was used for transformation of *E. coli* strain K17 (DE3). Replacement of one of three Cys by Trp and of another Cys by Ala produced ImmE1 with single Trp and single Cys side chains.

Overexpression of ImmE1. The *E. coli* strains BL21 (DE3) and K17 (DE3) were used for overexpression from the plasmid pT7Imm (*35*). Cells were grown at 37 °C to an $OD_{600} \sim 1.0$ in $2 \times$ YT media and incubated an additional 3 h following induction with 0.25 mM IPTG. Cells were harvested and stored at -20 °C until further use.

Isolation of Membrane Fractions. Frozen cell pellets from 4 L of culture were homogenized in 120 mL of medium containing 10 mM DMG, 100 mM KCl, pH 5.0 (buffer A). The suspension was brought to a final concentration of 1 mM PMSF, 1 mM DTT, and 1 mM EDTA and passed twice through a French Pressure cell at 1100 psi. Following centrifugation at 7000*g* (10 min), crude membrane fractions were isolated by centrifugation at 150000*g* (1 h) in a Ti60 rotor at 4 °C. The pellets were homogenized in 50 mL of 2 M NaBr, buffer A, 1 mM PMSF, and 1 mM DTT, and incubated on ice for 20 min prior to centrifugation as described above. The pellet was homogenized in 100 mL of buffer A, 1 mM PMSF, and 1 mM DTT and again centrifuged as described. Final pellets were homogenized in 30 mL of buffer A, 1 mM DTT, and stored at -20 °C until further use.

ImmE1 Purification. ImmE1 was extracted from NaBr-washed membranes by addition of an equal volume of 1-butanol at 4 °C and further incubation at 4 °C for 1−2 h with thorough mixing. Organic and aqueous phases were separated by centrifugation at 3000*g* at 4 °C, and the butanol (upper) phase was collected. The butanol phase was dried under rotary evaporation (-45 °C) and resuspended in 3 mL of chloroform/methanol/H_2O (4:4:1; solvent B). Subsequent chromatography was conducted at room temperature. Resuspended material was chromatographed on Sephadex LH-20-100 (30 $\times$ 2.5 cm) in solvent B at a flow rate of approximately 0.5 mL/min. ImmE1 was detected by absorption spectroscopy (320−240 nm). Pooled LH-20-100 fractions were adsorbed on a 30-mL CM-cellulose column previously equilibrated in solvent B. Protein was eluted in chloroform/methanol/H_2O/88% formic acid (4:4:0.6:0.4) after the column had been washed with approximately 50 mL of solvent B. Pooled fractions were concentrated by precipitation through the addition of 10 vol of diethyl ether and subsequent incubation on ice for 2 h. Precipitated protein was collected by centrifugation at 9000*g* (30 min, 4 °C), dried under a slow stream of N_2, and further dried under vacuum at room temperature for 1 h. Dried ImmE1 pellets were resolubilized in chloroform/methanol/H_2O (4:4:1), 50% TFE, or in 1-butanol/H_2O (20:1) with 10 mM ammonium acetate, pH 7.0.

SDS−PAGE and Purity of ImmE1. ImmE1 fractions were assessed for purity employing a modified Tris-Tricine gel system (*36*) with stacking and resolving gels of 3 and 12.5%, respectively. Stacking and resolving gels contained 0.5% SDS and the cathode buffer, 0.8% SDS, to help eliminate ImmE1 self-association during electrophoresis. Prior to electrophoresis, NaBr-washed membranes were brought to 200 mM NaOH, 2% SDS, and 1% β-mercaptoethanol, while samples in organic solvents were precipitated with 10 vol of diethyl ether, dried, and resuspended in 200 mM NaOH, 2% SDS, and 1% β-mercaptoethanol. Gels were stained with either silver (*37*) or Coomassie Brilliant Blue.

Pooled material following CM-cellulose was electrophoresed as described above and blotted onto PVDF membranes for identification and evaluation of purity with respect to protein by amino acid composition analysis. The amount of contaminating phospholipid was determined by quantitation of inorganic phosphate (*38*).

Circular Dichroism. All measurements were acquired at room temperature using a Jasco-600 spectropolarimeter. Quartz cells with a path length of 0.1 or 0.2 mm were used for far-UV measurements. Spectral parameters: time constant, 2 s; scan speed, 20 nm/min; scanning increment, 0.1 nm; spectral bandwidth, 2 nm. Spectra were recorded in 1-butanol/H_2O (19:1) at a protein concentration of 0.25 mg/mL. Secondary structure content was determined as an average of two methods of analysis of CD spectra in the 190−240 nm spectral range (*39*, *40*), compiled in the program PROT CD (*41*).

NMR Spectroscopy. Samples for NMR consisted of $\sim$100 μM wild type, unmodified C50A/C94W, or PROXYL-maleimidomethyl-modified C50A/C94W immunity protein in 100 μL of 4:4:1 $CDCl_3$/CD_3OH/H_2O. A 2.5-mm triple resonance Bruker microprobe with gradients in a Bruker DRX600 spectrometer was used to collect the data. Each experiment was recorded at 30 °C with a sweep width of 16 ppm. Solvent suppression was achieved using a double pulsed field gradient echo technique (*42*). For each spectrum, 4096 transients of 8192 data points were averaged.

PROXYL-maleimide modification of a single Cys mutant of ImmE1, C50A/C94W, was made in $CHCl_3$/CH_3OH/H_2O (3:3:1), containing 25 mM ammonium acetate, pH 7.0 (*23*, *43*). A total of 3 mg of ImmE1 was incubated with 3 mM PROXYL-maleimide for 2 h at 23 °C. The modified protein was separated from excess reagent on a Sephadex LH20 column in $CHCl_3$/CH_3OH/H_2O (4:4:1).

Gradient-enhanced two-dimensional $^1H^{15}N$ HSQC spectra (*44*) of ImmE1 expressed in minimal medium containing 1.0 g/L $^{15}NH_4Cl$ (*45*) were acquired with 2048 $\times$ 128 complex points in the direct and indirect dimensions, with 16 scans per t_1 increment. Sweep widths were 7788 Hz in the proton dimension and 2500 Hz in the nitrogen dimension. The two-dimensional data were processed and analyzed using NMR-PIPE (*46*). The ImmE1 protein was stable in chloroform/methanol/H_2O. There were no detectable changes in the HSQC spectra over the course of 7 days at 30 °C.

Analysis of ImmE1 Membrane Topology. ImmE1 was compared with the other five immunity proteins of the E-type channel-forming colicins (*1*): ImmE1*, Imm10, Imm5&K, ImmIa, and ImmIb. Patterns based on three conserved regions in ImmE1 (residues 4−14, 45−57, and 92−103, Figure 3) were used to search the SWISS-PROT and TrEMBL databases (ScanProsite, http://www.expasy.ch/tools/scnpsit2.html). Ten sequences were consistently found with all three conserved regions, here classified into five groups (SWISS-PROT or TrEMBL codes given): ImmE1: IMM0_ECOLI, IMM1_ECOLI, IMM1_SHISO, O87672 (from *Aeromonas hydrophila*); Imm10: Q47126; ImmK&5: IMMK_ECOLI; ImmIa: IMMI_ECOLI, Q46739, Q46741; ImmIb: IMMJ_ECOLI. These sequences were initially aligned using Clustal W (*47*) and slightly adjusted to produce more contiguous transmembrane segments, which did not change the alignment scores significantly. Transmembrane α-helices and topology were predicted using the programs TopPred II (*48*), MEMSAT,

setting the minimum helix length to 19 residues (*49*), PHD (*50*), and TMAP (*51*).

Spot-Test Assay of in Vivo ImmE1 Activity. E. coli K17 (DE3), harboring the plasmid pT7Imm, in which respective replacements in the Imm gene were made, were spread on Petri plates. A total of 20 μL of colicin E1 (3×10^{-9}–3×10^{-4} g/mL) in 0.1 M NaPi, pH 7.0, was overlaid, and plates were incubated at 37 °C.

RESULTS

Overexpression and Purification. Isolation of ImmE1 in quantities sufficient for characterization and structural analysis was complicated by low expression levels directed by the natural plasmid pColE1. Overexpression of ImmE1 from the pT7-7 promoter resulted in an approximately 50-fold increase in yield to ∼1 mg/L cells. Efforts to further increase expression levels using different promoters (*tac* and T7) in several constructs (native ImmE1, GST-ImmE1, and His6-ImmE1) and bacterial strains [RB791, LM101, JM103, JM105, BL21, BL21(DE3), and BL21(DE3)LysS] did not increase the yield of ImmE1, suggesting that the above levels may represent a ceiling for expression (*35*). These results are consistent with a previous study reporting production of ImmE1 from a plasmid under control of the *tac* promoter (*52*). The limited success encountered in following the conventional approach of screening a variety of different detergents and chromatographic procedures for purification of ImmE1 (ref *35*; R. Taylor, unpublished data) led to investigation of the use of organic solvents as an alternative medium for isolation and purification.

The level of ImmE1 purity in the stages of membrane isolation, extraction, and chromatographic separation is shown (Figure 1, panel A). Comparison of the butanol extract with isolated membrane fractions demonstrates the unique solubility profile of ImmE1, as only trace contaminants are observed after a single membrane extraction step. Following transfer of the butanol-soluble material into a chloroform/methanol/H$_2$O (4:4:1, v/v) solvent system, the ImmE1 was purified to apparent homogeneity by gel filtration on Sephadex LH-20-100, followed by CM-cellulose chromatography. Final purity of ImmE1 with respect to protein was confirmed by amino acid composition analysis (Figure 1, panel B) and determination of a unique N-terminal sequence (NH$_2$-M–S–L–R–Y–Y-). Determination of inorganic phosphate indicated only trace amounts of phospholipid following chromatography on Sephadex LH-20-100 (not shown).

Secondary Structure Analysis by Circular Dichroism. The far-UV circular dichroism spectrum of ImmE1 in 1-butanol or 50% TFE (Figure 2), showing minima at 208 and 222 nm, and a large peak of positive ellipticity centered at approximately 193 nm, is characteristic of α-helical proteins (*41*). Analysis of the spectra (*39*, *40*) yielded an estimate of 79 and 77% α-helical content in 1-butanol and 50% TFE, respectively. This spectroscopic analysis is the first empirically derived secondary structure analysis for the hydrophobic immunity proteins of the channel-forming colicins. It was not possible to obtain far-UV CD spectra below 250 nm in chloroform-containing solvents, which were useful for NMR structural studies, because of high optical density. Spectra were also measured in SDS micelles, in which the α-helical content was 55% (data not shown).
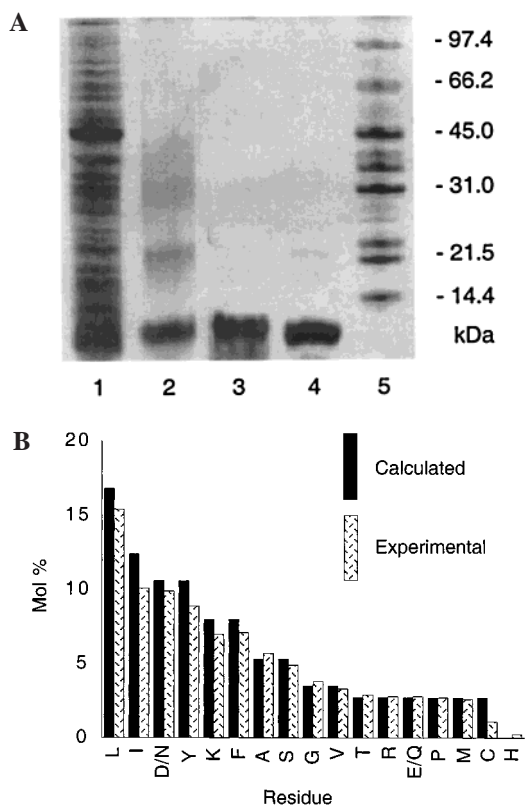

FIGURE 1: Extraction, purification, and identification of ImmE1. (A) Protein detected by silver staining following separation on a 12.5% SDS−polyacrylamide gel. Lane 1, isolated membranes following extraction with 2 M NaBr; lane 2, organic phase following butanol extraction of NaBr washed membranes; lane 3, pooled fractions following Sephadex LH 20-100; lane 4, pooled fractions following CM-cellulose; lane 5, low molecular weight protein standards. (B) Comparison of ImmE1 amino acid composition calculated from the primary sequence (solid bars) with that determined for pooled fractions following CM-cellulose (hatched bars).
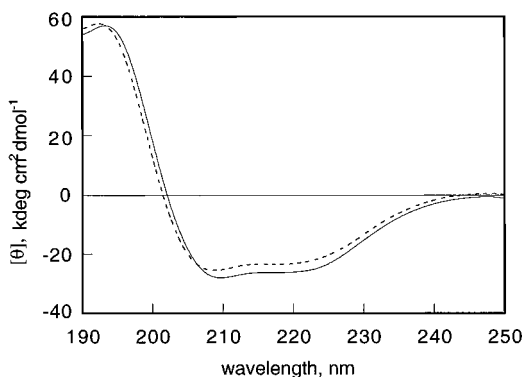

FIGURE 2: Far-UV circular dichroism spectrum of wild-type ImmE1. The purified ImmE1 was solubilized in 1-butanol/H$_2$O, 19:1 v/v (solid), or 50% TFE (dashed). The secondary structure content, inferred from the analysis of the far-UV CD spectra in 1-butanol or TFE, was α-helix, 79 or 77%; β-sheet, 10 or 9%; β-turns, 3 or 3%; remainder, 8 or 10%, respectively.

Prediction of ImmE1 Membrane Topology. ImmE1 is related to the immunity proteins ImmE1*, Imm10, Imm5&K, ImmIa, and ImmIb (*1*). An alignment of the six known E-type immunity proteins (Figure 3) shows a high conservation of the three extended hydrophobic regions (dark, shaded), inferred to be transmembrane α-helices in the hydrophobic core region of the membrane (dark, shaded),

```
           10        20
ImmE1   1 M----SLRYYIKNI LFGLYCYLIY IYLITKNSEG 30
ImmE1*  1 M----SLRYYIKNI LFGLYCALIY IYLITKNNEG 30
Imm10   1 M----TVKYYLHNL LESLIPWLFY LLLNYKT--- 27
Imm5&K  1 M----HLKYYLHNL PESLIPWILI LIFNDND--- 27
ImmIa   1 MN----RKYYFNNM WWGWVTGGYM LYMSWDYEKF 30
ImmIb   1 MKLDISVKYLLKSL IPILIILTVF YLGWKDNQEN 34
```
                    Helix 1

```
           40        50        60
ImmE1  31 YYFLVSDKML YAIVISTILC PYSKYAIEYA AFNAIKKDFF 70
ImmE1* 31 YYFLASDKML YAIVISTILC PYSKYAIEHI FFKFIKKDFF 70
Imm10  28 ---PPFSLII FIASIHVLLY PYSKLTIFSF IQNTTKMKKE 64
Imm5&K 28 ---NTPLLFI FISSIHVLLY PYSKTLISRY IKENTKLKKE 64
ImmIa  31 ----YRLLFW CISLCGMVLY PVAKWYIEDT ALKFTRPDWF 66
ImmIb  35 ---ARMFYAF IGCIISAITF PFSMRIIQKM VIRFTGKEFW 71
```
                    Helix 2

```
           80        90        100       110
ImmE1  71 ERRKNLNNAP VAK-LNLFMLY NLLCLVLAIP FGLLGLFISI -KNN 113
ImmE1* 71 RRKRKNLNKCP RGKIKPYLCVY NLLCLVLAIP FGLLGLVYIN -KE  113
Imm10  65 ---------- ---PWYSYNLF YFLYLAMAIP VGLPSFIYYS LKRN  96
Imm5&K 65 ---------- ---PWYLCKLS ALFYLLMAIP VGLPSFIYYT LKRN  96
ImmIa  67 NSGPFAD--- TPGKMGLLAVY TGTVFILSLP LSMIYILSVI IKRLSVR 111
ImmIb  72 QKDFFTN--- -PVGGSLTAIF ELFCFVISVP VVAIYLIFIL CKALSGK 115
```
                    Helix 3

FIGURE 3: Primary sequence analysis of the six E-type immunity proteins. Alignment of the E-type immunity proteins showing the consensus prediction for the three extended hydrophobic domains, consistently predicted to be in the hydrophobic membrane core (gray bars underneath sequences). Residues near the helix ends that were inconsistently predicted to be in the membrane core, and are inferred to be in the membrane interfacial layer (Figure 4), are indicated by bold letters. Numbering according to the ImmE1 sequence.

from both the sequence pattern and gene fusion analysis (*2*). The light shaded region of the schematic membrane shown in Figure 4 represents the membrane interfacial layer that has an intermediate dielectric constant (*53*, *54*). Advantage was taken of the conservation of hydrophobic domains to derive a more precise topology model for ImmE1 by employing four predictive methods, TopPred II (*48*), MEM-SAT (*49*), PHD (*50*), and TMAP (*51*), across the six immunity protein sequences. The transmembrane helix ends predicted by these four algorithms agreed to within 1−2 residues of standard deviation (Table 2). The consensus prediction agrees well with the existence of three transmembrane α-helices, extending between residues 6−26, 37−57, and 88−109 for H1, H2, and H3, respectively. This is consistent with ca. 80% helical content (Figure 2) and a cytoplasmic location of the N-terminus inferred from the gene fusion studies (*2*). However, this results in a substantial modification of the previous topology model of ImmE1 that predicted helices H1−H3 to be composed of residues 9−28, 44−65, and 84−105, respectively (*2*). The 178-residue hydrophobic immunity protein, ImmA, associated with the channel-forming colicin A, has been inferred from genetic analysis, to have four transmembrane helices (*55*).

In accord with the preference for Trp and Tyr residues of integral membrane proteins for the ends of transmembrane α-helices in the membrane interfacial regions (*54*, *56*, *57*), the ImmE1 topology model shows that two Tyr residues are probably located near the periplasmic and five Tyr located in or near the cytoplasmic membrane interface. However, it is predicted that five Tyr residues are located closer to the center of the bilayer (Figure 4, panel A). Three of the latter group, Y15, Y20, and Y22, are located in transmembrane helix H1, and two, Y41 and Y52, in H2. These residues will be discussed below as candidate probes for the active versus inactive conformation of ImmE1.
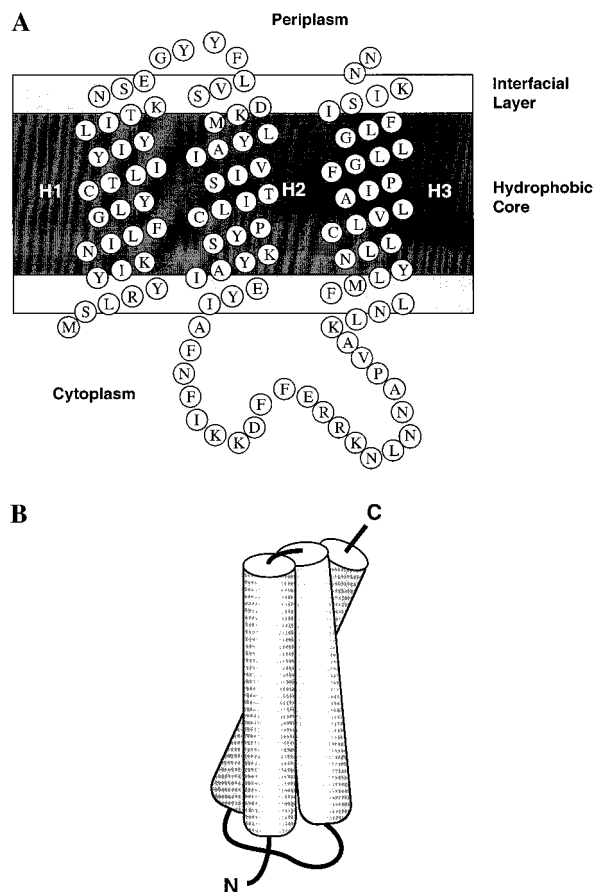

FIGURE 4: Topology model of the colicin E1 immunity protein. (A) Multisource hydropathy (*44*, *45*) and topology analysis (*45*−*48*) of all six immunity proteins to pore-forming colicins were employed for prediction of helix ends. Dark and lightly shaded regions represent the bilayer core and membrane interfacial layer, respectively. H1−H3, proposed transmembrane α-helices. There is a small discrepancy between the start of H3 in the bilayer core domain and that shown in Figure 3 because of the greater length of H3. (B) Model for interhelix interactions of transmembrane helices H1−H3 inferred from near-UV CD spectra and the Cys16-PROXYL quenching of Hε1 of the Trp94 indole ring. The interhelix tilt angles are drawn somewhat arbitrarily, with the awareness that the interhelix and helix-membrane normal tilt angles should be <20° and 40° (*51*). The relatively long H2−H3 loop is shown.

Table 2: Predicted Helical Ends for ImmE1 Membrane Topology Model Generated Using Four Methods for Alignment of Six E-Type Immunity Proteins

method	H1-N	H1-C	H2-N	H2-C	H3-N	H3-C
TopPred 11	5[a]	25	36	56	90	110
MEMSAT	8	25	39	59	86	108
PHD	14[b]	23	38	57	87	109
TMAP	7	27	35	55	87	112
average	7 ± 2	25 ± 1	37 ± 2	57 ± 2	87 ± 2	110 ± 2

[a] Numbering is according to the ImmE1 sequence. [b] Outlier excluded from calculations.

Evidence for a Compact, Folded ImmE1 Species in Chloroform/Methanol/H_2O *from Near-UV Circular Dichroism Spectra.* The near-UV CD spectra of ImmE1 were similar in H_2O-saturated 1-butanol (butanol/H_2O, 19:1, v/v) and in chloroform/methanol/H_2O (4:4:1). Wild-type ImmE1 has 9 Phe and 12 Tyr residues but no Trp. Therefore, negative CD signals in the 270−285-nm region originate from Tyr side chains only, whereas the sharp peaks in the 260−270-nm region could originate from Phe (Figure 5 red). All these
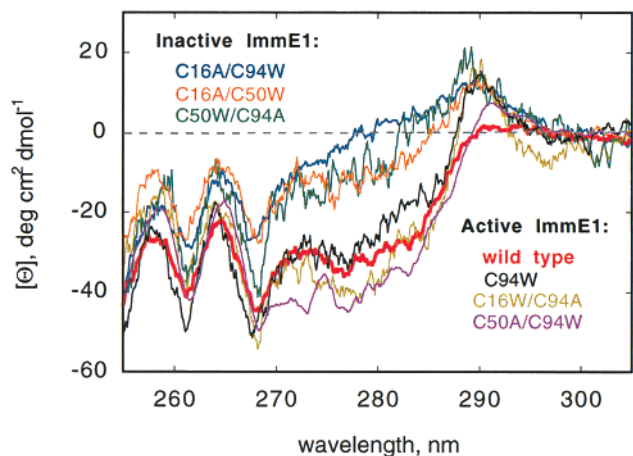
FIGURE 5: CD spectra of wild-type and mutant ImmE1 in the near-UV region. Spectra were taken in a chloroform/methanol/H₂O (4:4:1) solvent system at 23 °C of ImmE1 mutant proteins in which Cys at positions 16, 50, and/or 94 were substituted to Ala and/or Trp. Spectra of wild type (bold red), C94W (black), C16A/C94W (blue), C16A/C50W (orange), C16W/C94A (brown), C50A/C94W (violet), and C50W/C94A (green) ImmE1 are shown.

signals are overlaid with the long wavelength edge of the far-UV CD spectrum arising from α-helical secondary structure. The near-UV spectra for the wild type and the C50A/C94W and C16A/C94W mutants are stable for more than one week (data not shown).

To test tertiary structure and folding of isolated ImmE1 in organic solvents using CD and NMR spectoscopies, single Cys mutants were made by substitution of Cys 16, 50, or 94 to Ala or Trp in the extended hydrophobic domains H1−H3 (Figures 3 and 4). The absence of tryptophan residues in wild-type ImmE1 allowed designated sites in the primary sequence to be used as indicators of tertiary structure by site-specific introduction of a single tryptophan residue. All three Cys residues in ImmE1 were predicted to be in the hydrophobic core of the membrane bilayer (Figure 4). The C94W replacement resulted in the appearance of a positive CD signal at 290 nm (Figure 5, black), implying that Trp94 is constrained by neighboring groups. Similar signals appeared in C16W or C50W mutants. The C16A/C94W mutant (Figure 5, blue) has spectral characteristics similar to wild type, ImmE1, in the 250−270-nm region and a positive CD signal at 290 nm that belongs to the single Trp residue. However, the negative signals in the 270−285-nm region are significantly weaker than in the wild-type ImmE1, implying that some Tyr side chains have lost their constrained state as result of the two side chain replacements in hydrophobic domains H1 and H3. A similar decrease in this signal was detected in the C16A/C50W and C50W/C94W mutants (Figure 5, orange, green), whereas the spectra of C94A/C16W and C50A/C94W in the 270−280-nm region (Figure 5, brown, violet) were similar to that of the wild-type Imm.

"Spot" Test of in Vivo ImmE1 Activity. The set of single and double Cys mutants were tested for the protective activity of ImmE1 against the cytotoxic effect of added colicin, assayed through the extent of cell growth in the presence of exogenous colicin E1 ("spot" tests). The mutants varied substantially in their level of protective activity against colicin E1 (Table 3). C16A/C94W was the least active mutant. It was essentially inactive since the same small

Table 3: Spot-Test Assay of in Vivo Activity of Wild-Type and Mutant ImmE1 in Protection of Susceptible Cells against Colicin E1[a]

	colicin E1 concentration, 3× (g/mL)					
mutant	10^{-9}	10^{-8}	10^{-7}	10^{-6}	10^{-5}	10^{-4}
WT	+	+	+	+	+	+
C16A/C50W	+	+/−	−	−	−	−
C16A/C94W	+/−	−	−	−	−	−
C50A/C16W	+	+	+	+	+	+
C50A/C94W	+	+	+	+	+	+
C94A/C 16W	+	+	+	+	+	+
C94A/C50W	+	+	+/−	−	−	−
C16A/C50A	+	+	+	+	+	+
C16A	+	+	+	+	+	+
C94W	+	+	+	+	+	+

[a] *E. coli* K17 (DE3), harboring plasmid pT7-7Imm, in which respective replacements in the Imm gene were made, were spread on Petri plates. A total of 20 μL of colicin E1 in 0.1 M NaPi, pH 7.0, of the indicated concentration was overlaid before plates were incubated at 37 °C. Signs (+) or (−) indicate the presence or absence of activity, i.e., growth, in the spots to which colicin E1 was applied.

amount of colicin E1 (6 pg) as in the absence of the *imm* gene was sufficient to kill cells. Slightly weaker immunity "by-pass" effects were observed with C16A/C50W and C50W/C94A. No other combination of singleCys/singleTrp mutants or mutants with single replacements, C16A or C94W, impaired the functional activity of Imm (Table 3).

Comparison of the level of protective activity in the mutants with their corresponding CD spectra in the near-UV revealed a correlation between (a) the amplitude of the CD signal in the 270−285-nm region and (b) the in vivo activity of ImmE1: the greater the activity, the larger the amplitude of the negative signals in the 270−285-nm region of the spectrum.

Evidence from NMR for ImmE1 Folding in Chloroform/Methanol-H₂O. A one-dimensional spectrum of the upfield methyl region shows at least four methyl resonances that are shifted upfield, presumably by interaction with ring currents from aromatic residues that would be expected in a stably folded protein (Figure 6, panel A). Two-dimensional HSQC NMR spectra of an ¹⁵N-labeled protein provide a useful fingerprint of nearly every residue in the protein. From the range of amide chemical shifts, one can distinguish folded from unfolded proteins. From the ability to observe complete sets of cross-peaks even with short acquisition times, one can infer amenability of the sample to a full structural study. Two-dimensional ¹H¹⁵N HSQC spectra of uniformly ¹⁵N-labeled wild-type ImmE1 protein in chloroform/methanol/H₂O show the chemical shift dispersion (Figure 6, panel B) typical of folded membrane proteins (*12, 13*), which is also diagnostic of highly helical proteins. Despite the somewhat limited range of the chemical shifts, 95 of the expected 109 backbone amide cross-peaks can be resolved in the two-dimensional spectra if they are magnified by approximately 5-fold (not shown). The protein was sufficiently stable under these sample conditions for a complete structural study. HSQC spectra recorded before and after a one-week incubation at 30 °C were identical with respect to both cross-peak intensities and their locations.

Additional evidence for a folded structure of ImmE1 in chloroform/methanol/H₂O was obtained by NMR analysis of the active single Cys mutant of ImmE1 (C50A/C94W),
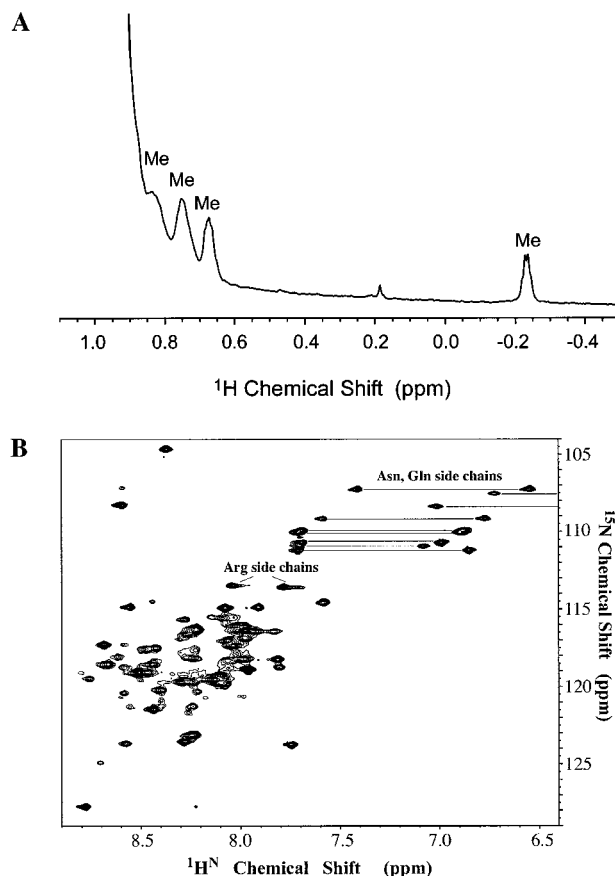
A

B

FIGURE 6: NMR spectra of wild-type ImmE1. (A) Upfield region of the ^{1}H NMR spectrum of ImmE1 (50 μM) in 4:4:1 CDCl$_3$/CD$_3$-OH/H$_2$O. Several methyl resonances, labeled at -0.25, 0.67, 0.76, and 0.82 ppm, are shifted upfield from the approximate position of $0.9-1.15$ ppm associated with unshifted methyl groups of aliphatic residue side chains, reflect long-range contacts with aromatic side chains elsewhere in the protein and are indicative of a stably folded structure. (B) Two-dimensional ^{1}H^{15}N HSQC NMR spectrum (600 MHz) of uniformly ^{15}N-labeled ImmE1 protein (0.3 mM) in 4:4:1 CDCl$_3$/CD$_3$OH/H$_2$O. The amide protons show the limited chemical shift dispersion typical for membrane proteins (*12*, *13*), consistent with both a highly helical structure as well as the folded helical structure of a membrane protein. About 95 of the expected 109 backbone amide cross-peaks can be resolved when the spectrum is expanded 5-fold (not shown).

containing a spin label probe attached to Cys-16 near the middle of the central transmembrane domain, H1 (Figure 3). The indole Hϵ1 of the single Trp was identified by comparison with the spectrum of the wild-type protein. While the indole proton resonance was readily observed for the C50A/C94W mutant that was not modified with a spin label, this resonance was broadened beyond detection in the presence of the PROXYL spin label (Figure 7). The ability of the spin label to broaden the indole proton resonance demonstrates that the spin label and Trp-94 are separated by ≤12 Å in space (*40*), although they are separated by 77 residues in primary sequence. Hence, the protein must adopt a stable tertiary fold that brings these two residues into proximity.

Line Width and Oligomeric State. The line width, $13-17$ Hz, of the amide and alpha ^{1}H resonances of the 13-kDa ImmE1 protein in the organic solvent mixture, as compared to line widths of $\sim$13, 25, and 35 Hz for proteins of molecular mass 8.5, 24, and 30 kDa, clearly indicates that the protein is monomeric under these conditions.
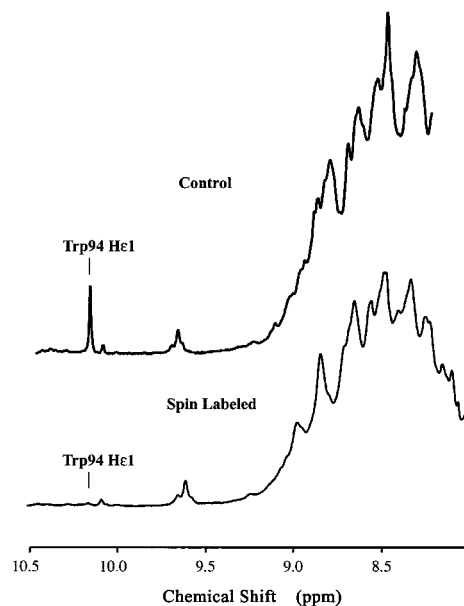

FIGURE 7: Broadening of indole NH region of Trp94 by spin label adduct of Cys16. Upper panel: Control, showing the indole H-1 of the Trp94 ImmE1 mutant. Lower panel: PROXYL-modified Cys50Ala/Cys94Trp ImmE1, showing the loss of the indole spectrum in the presence of PROXYL-modified Cys16. The extent of the relaxation effect indicates that the nitroxide radical attached to Cys16 and the Trp94 indole side chain are within $10-15$ Å of each other.

DISCUSSION

The Folded State of ImmE1. In light of the seemingly harsh conditions used throughout the purification of ImmE1 in organic solvents, it is critical to gain information on the folded state of the molecule in these potentially membrane mimetic but diverse and poorly understood environments. The following spectral information was obtained: (i) From the CD spectrum of wild-type ImmE1 in the $270-285$ nm region, assigned to Tyr, some Tyr side chains were inferred to be constrained by interhelix interactions. It should be noted that, on the basis of the relative extinction coefficient of Tyr versus Trp, the amplitude of the Tyr near-UV CD spectra (ca. 35 deg cm^2 dmol^{-1}) is quite significant for wild-type ImmE1 and the active mutants. (ii) The near-UV CD band at 290 nm in the Cys $\rightarrow$ Trp mutants (Figure 5) implies that the Cys residues in the hydrophobic domains of the three transmembrane helices (Figure 4, panel A) are in a constrained environment. (iii) The quenching of the Hϵ1 indole resonance of Trp 94 by spin labeled Cys16 implies that the spin label and the indole ring are separated by <12 Å. It is not known whether this distance is dependent on Imm activity. (iv) The correlation between loss of ImmE1 activity and perturbation of the Tyr region of the spectrum, as a result of mutational changes in two of the three long hydrophobic transmembrane helices, implies a wild-type conformation involving helix$-$helix interactions, perhaps in a crossed helical bundle with complementary interactions between the three helices (Figure 4, panel B). The correlation between near-UV CD spectral changes attributed to Tyr residues (Figure 5) and ImmE1 activity (Table 3) is an unprecedented application of this spectroscopic method. Of the 12 Tyr in the protein, it can be seen in the ImmE1 topology model (Figure 4, panel A) that five residues, Y15, Y20, Y22, Y41, and Y52, lie within one helical turn of the center of the

bilayer in the putative transmembrane helices H1 and H2. Since the above spectroscopic data (i−iii), including the correlation of near-UV CD with activity (iv), imply helix−helix interactions in or near the hydrophobic core, these five Tyr are candidates for the residues whose constraints induce the near-UV CD signals.

Analysis of the nature of the folded state by NMR and near-UV CD spectroscopy, and of the protective activity of the immunity protein against colicin cytotoxicity, implied a folded ImmE1 conformation in the chloroform/methanol/H$_2$O solvent system. The spectroscopic data (i−iv) supply additional detail to the membrane folding pattern of ImmE1. In addition to three transmembrane helices shown in Figure 4, panel A, the CD data imply that helices H1−H3 interact near the center of the bilayer (Figure 4, panel B). From the correlation between ImmE1 activity and near-UV CD data (Figure 5), it was inferred that the details of these interactions are a determinant of activity. These results, together with the 2D HSQC spectrum (Figure 6), provide the experimental evidence necessary to rationalize a full structural analysis by multidimensional NMR studies of the ImmE1 protein solubilized in this membrane-mimetic organic solvent mixture.

Point Mutants of ImmE1. No single point mutation, including T17K, I19K, I21K, M39K, I43K, and I45K, studied previously (2), has been found that causes any measurable inactivation of ImmE1, showing that this integral membrane protein preserves its transmembrane hydrophobic domains (helices) after insertion of an unpaired (uncompensated) charged side chain into these domains. In the present study, C16A and C94W were also found to be innocuous. In ref 2 and in the present study, ImmE1 could be inactivated by double mutations. The lack of inactivation of ImmE1 by single residue substitutions, including insertion of lysine residues in the hydrophobic transmembrane helices, implies that the helices are stabilized by mutual interactions in addition to those between hydrophobic helices and lipids. This increased stability is consistent with additional stabilization conferred by helix−helix interactions. Double substitution of residues in different helices and insertion of such bulky residues as Trp at positions critical for interhelix interactions probably impairs those interactions to an extent sufficient to inactivate ImmE1 function. This substitution is not sufficient to break the interhelix contacts completely, as seen in the preservation of the near-UV CD signal from Trp94 at 290 nm in the C50A/C94W mutant (Figure 5). However, loosening of the interhelix contacts is sufficient to impair the constrained state of the less bulky aromatic residue, Tyr. The identification of the tyrosines responsible for double-mutation-sensitive CD signals in the 270−280-nm region should provide information on interhelix contacts and interactions crucial for ImmE1 function.

Solubility, Folding in Solvents of Mixed Polarity; Protein Properties. The specific structural features that confer organic solvent solubility on selected integral membrane proteins remain unclear. The selective solubilization, from the entire set of *E. coli* membrane proteins after NaBr extraction, of ImmE1 in 1-butanol (Figure 1, panel A, lane 2 vs lane 1) demonstrates that such solubility is an unusual property even for hydrophobic, integral membrane proteins. It has been previously noted that the unique solubility of ATPase proteolipid subunit *c* and EmrE in mixed polarity solvents

is not likely to stem from an unusually large proportion of hydrophobic amino acids (44 and 49%, respectively) relative to other ion-coupled transporters (41−50%), but that the low incidence of unpaired charges may be the most critical parameter for solubilization (11). ImmE1 appears to represent a slightly different situation, as inspection of the primary sequence shows ImmE1 to be both less hydrophobic than EmrE and to carry a formal net charge of +7 at neutral pH (Table 1). Thus, from the studies on ImmE1, the critical parameters for solubility in organic solvents include (i) a low molecular weight (ca. 10 000), (ii) a hydrophobic primary sequence, and (iii) a tendency to form extended (ca. 20−25 residues) α-helices in a low dielectric environment.

Far-UV CD secondary structure analysis indicates that ImmE1 adopts a predominantly α-helical conformation in a membrane-mimetic environment (Figure 2). Although co-solvents such as methanol and TFE are commonly considered as generically helix-promoting, β-sheet (30), β-turn (58), and mixed α/β-structures (29) have also been observed in their presence. A more detailed analysis of water-soluble proteins suggests such solvents are helix-stabilizing only for regions of primary sequence with a significant inherent helical propensity (28). Considering the dependence of the helical propensity of membrane proteins on solvent polarity (59), cosolvents provide an important opportunity to compare the properties of water-soluble and integral membrane proteins in common environments for cases where their solubility profiles overlap. For soluble proteins, the secondary structure elements observed in the presence of cosolvents have been proposed to be those present during the hydrophobic collapse that occurs early in the folding pathway, and hence the "alcohol-denatured state" may be diagnostic of a kinetic intermediate in the folding pathway (28−31). The two-state model for membrane protein folding postulates that individual transmembrane α-helices are inserted into the bilayer as independent structural domains that subsequently form tertiary contacts through specific helix−helix interactions that determine the native fold (60, 61). Thus, the delineation of the secondary structure elements of proteins such as BR, DAGK, and EmrE is of interest in the context of understanding the kinetic intermediates in the poorly understood process of membrane protein folding.

ACKNOWLEDGMENT

REFERENCES

1. Cramer, W. A., Heymann, J. B., Schendel, S. L., Derity, B. N., Cohen, F. S., Elkins, P. A., and Stauffacher, C. V. (1995) *Annu. Rev. Biophys. Biomol. Struct. 24*, 611−641.
2. Song, H. Y., and Cramer, W. A. (1991) *J. Bacteriol. 173*, 2935−2943.
3. Cramer, W. A., Lindeberg, M., and Taylor, R. (1999) *Nat. Struct. Biol. 6*, 295−297.
4. Zhang, Y.-L., and Cramer, W. A. (1993) *J. Biol. Chem. 268*, 10176−10184.
5. Garavito, M. R., Picot, D., and Loll, P. J. (1996) *J. Biomem. Bioenerg. 28*, 13−27.
6. Michel, H. (1997) *Trends Biochem. Sci. 8*, 56−59.

7. Beechey, R. B., Linnett, P. E., and Fillingame, R. H. (1979) *Methods Enzymol. 55*, 427−434.

8. Bohnenberger, E., and Sanderman, H. (1979) *Eur. J. Biochem. 94*, 401−407.

9. Sigrist-Nelson, K., and Azzi, A. (1979) *Biochem. J. 177*, 687−692.

10. Boyot, P., Luu, B., Jones, L. R., and Trifilieff, E. (1989) *Arch. Biochem. Biophys. 269*, 639−645.

11. Yerushalmi, H., Lebendiker, M., and Schuldiner, S. (1995) *Biol. Chem. 270*, 6856−6863.

12. Girvin, M. E., Rastogi, V. K., Abildgaard, F., Markley, J. L., and Fillingame, R. H. (1998) *Biochemistry 37*, 8817−8824.

13. Schwaiger, M., Lebendiker, M., Yerushalmi, H., Coles, M., Groger, A., Schwarz, C., Schuldiner, S., and Kessler, H. (1998) *Eur. J. Biochem. 254*, 610−619.

14. Vinogradova, O., Badola, P., Czerski, L., Sonnichsen, F. D., and Sanders, C. R. (1997) *Biophys. J. 72*, 2688−2701.

15. Pervushin, K. V., Orekhov, V. Y., Popov, A. I., Mushina, L. Y., and Arseniev, A. S. (1994) *Eur. J. Biochem. 219*, 571−583.

16. Schuldiner, S., Lebendiker, M., and Yerushalmi, H. (1997) *J. Exp. Biol. 200*, 335−341.

17. Torres, J., and Padros, E. (1993) *FEBS Lett. 318*, 77−79.

18. Smith, R. L., O'Toole, J. F., Maguire, M. E., and Sanders, C. R. (1994) *J. Bacteriol. 176*, 5459−5465.

19. Engelman, D. M., Steitz, T. A., and Goldman, A. (1986) *Annu. Rev. Biophys. Biophys. Chem. 15*, 321−353.

20. Sanders, C. R., Czerski, L., Vinogradova, O., Badola, P., Song, D., and Smith, S. O. (1996) *Biochemistry 35*, 8610−8618.

21. Wallace, B. A., and Teeters, C. L. (1987) *Biochemistry 26*, 65−70.

22. Girvin, M. E., and Fillingame, R. H. (1994) *Biochemistry 33*, 665−674.

23. Girvin, M. E., and Fillingame, R. H. (1995) *Biochemistry 34*, 1635−1645.

24. Jones, P. C., Jiang, W., and Fillingame, R. H. (1998) *J. Biol. Chem. 273*, 17178−17185.

25. Rastogi, V. K., and Girvin, M. E. (1999) *Nature 402*, 263−268.

26. Jiang, W., and Fillingame, R. H. (1998) *Proc. Natl. Acad. Sci. U.S.A. 95*, 6607−6612.

27. Gratias, R., and Kessler, H. (1998) *J. Phys. Chem. B, 102*, 2027−2031.

28. Buck, M., Schwalbe, H., and Dobson, C. M. (1995) *Biochemistry 34*, 13219−13232.

29. Harding, M. M., Williams, D. H., and Woolfson, D. K. (1991) *Biochemistry 30*, 3120−3128.

30. Schonbrunner, N., Wey, J., Engels, J., Georg, H., and Kiefhaber, T. (1996) *J. Mol. Biol. 260*, 432−445.

31. Fan, P., Bracken, C., and Baum, J. (1993) *Biochemistry 32*, 1573−1582.

32. Luo, P., and Baldwin, R. L. (1997) *Biochemistry 36*, 8413−8421.

33. Kyte, J., and Doolittle, R. F. (1982) *J. Mol. Biol. 157*, 105−132.

34. Fisher, C. L., and Pei, G. K. (1997) *BioTechnique 23*, 570−574.

35. Heymann, J. B. (1995) Ph.D. Thesis, Purdue University.

36. Schaegger, H., and Von Jagow, G. (1987) *Biochemistry 166*, 368−379.

37. Blum, H., Beier, H., and Gross, H. J. (1987) *Electrophoresis 8*, 93−99.

38. Jaenicke, L. (1974) *Anal. Biochem. 61*, 623−627.

39. Provencher, S. W., and Glockner, J. (1981) *Biochemistry 20*, 33−37.

40. Chang, T. C., Wu, C.-S. C., and Yang, J. T. (1978) *Anal. Biochem. 91*, 13−31.

41. Venyaminov, S. Y., and Yang, J. T. (1996) in *Circular Dichroism and the Conformational Analysis of Biomolecules* (Fasman, G. D., Ed.) pp 69−107, Plenum, New York.

42. Hwang, T. L., and Shaka, A. J. (1995) *J. Magn. Reson. Ser. A., 112*, 275−279.

43. Kosen, P. A. (1989) in *Methods in Enzymology,* Vol. 177, (Oppenheimer, N. J., James, T. L., Eds.) pp 86−121, Academic Press, New York.

44. Kay, L. E., Keifer, P., and Saarinen, T. (1992) *J. Am. Chem. Soc. 114*, 10663−10665.

45. Kim, Y., Valentine, K., Opella, S. J., Schendel, S. L., and Cramer, W. A. (1998) *Protein Sci. 7*, 342−346.

46. Delaglio, F., Grzesiek, S., Vuister, G. W., Zhu, G., Pfeifer, J., and Bax, A. (1995) *J. Biomol. NMR 6*, 277−293.

47. Thompson, J. D., Higgins, D. G., and Gibson, T. J. (1994) *Nucleic Acids Res. 22*, 4673−4680.

48. Claros, M.-G., and von Heijne, G. (1994) *CABIOS, Comput. Appl. Biosci. 10*, 685−686.

49. Jones, D. T., Taylor, W. R., and Thorton, J. M. (1994) *Biochemistry 33*, 3038−3049.

50. Rost, B., Casadio, R., Fariselli, R., and Sander, C. (1995) *Protein Sci. 4*, 521−533.

51. Persson, B., and Argos, P. (1994) *J. Mol. Biol. 237*, 182−192.

52. Shirabe, K., Yamada, M., Merrill, A. R., Cramer, W. A., and Nakazawa, A. (1993) *Plasmid 29*, 236−240.

53. Cherepanov, D. I., and Krishtalik, L. I. (1990) *Bioelectrochem. Bioenerg. 24*, 113−127.

54. Wimley, W. C., and White, S. H. (1996) *Nat. Struct. Biol. 3*, 842−848.

55. Geli, V., Baty, D., Pattus, F., and Lazdunski, C. (1989) *Mol. Microbiol. 3*, 679−687.

56. Wallin, E., Tsukihara, T., Yoshikawa, S., von Heijne, G., and Elofsson, A. (1997) *Protein Sci. 6*, 808−815.

57. Reithmeier, R. (1995) *Curr. Opin. Struct. Biol. 5*, 491−500.

58. Blanco, F. J., Jimenez, A., Pineda, A., Rico, J., and Nieto, J. L. (1994) *Biochemistry 33*, 6004−6014.

59. Liu, L.-P., and Deber, C. M. (1998) *J. Biol. Chem. 37*, 23645−23648.

60. Popot, J.-L., and Engelman, D. M. (1990) *Biochemistry 29*, 4031−4037.

61. Lemmon, M. A., and Engelman, D. M. (1994) *Q. Rev. Biophys. 27*, 157−218.